Title

How Do Radionuclides Accumulate in Marine Organisms? A Case Study of Europium with Aplysina cavernicola

Journal

Environmental Science and Technology, 50(19)

ISSN

0013-936X

Authors

Maloubier, Melody

Shuh, David K

Minasian, Stefan G

et al.

Publication Date

2016-10-04

DOI

10.1021/acs.est.6b01896

How do radionuclides accumulate in marine organisms? A case study of europium with *Aplysina cavernicola*

Melody MALOUBIER[a,b], David K. SHUH[c], Stefan G. MINASIAN[c], Joseph I. PACOLD[c], Pier-Lorenzo SOLARI[d], Hervé MICHEL[a], François R. OBERHAENSLI[e], Yasmine BOTTEIN[e], Marguerite MONFORT[b], Christophe MOULIN[b], Christophe DEN AUWER[a*]*

[a] Université Côte d'Azur, CNRS, Institut de Chimie de Nice, 06108, Nice, France

[b] CEA, DAM, DIF, F-91297 Arpajon, France

[c] Chemical Sciences Division, Lawrence Berkeley National Laboratory, Berkeley, California 94720

[d] Synchrotron SOLEIL L'Orme des Merisiers, Saint-Aubin, BP 48, F-91192 Gif-sur-Yvette Cedex, France

[e] IAEA, Environment Laboratory, 4 Quai Antoine I[er], MC-98000, Monaco

Corresponding authors

- Christophe Den Auwer, christophe.denauwer@unice.fr, Université Côte d'Azur, CNRS, Institut de Chimie de Nice, France. Phone : +33 4 92 07 63 62

- Christophe Moulin, christophe.moulin@cea.fr, CEA, DAM, DIF, F-91297 Arpajon. Phone : + 33 1 69 26 59 70

Abstract:

In the ocean, complex interactions between natural and anthropogenic radionuclides, seawater and diverse marine biota provide a unique window through which to examine ecosystem and trophic transfer mechanisms in case of accidental dissemination. The nature of interaction between radionuclides, the marine environment and marine species is therefore essential for better understanding the transfer mechanisms from the hydrosphere to the biosphere. Although data pertaining to the rate of global transfer is often available, little is known regarding the mechanism of environmental transport and uptake of heavy radionuclides by marine species.

Among marine species, sponges are immobile active filter feeders and have been identified as hyper accumulators of several heavy metals. We have selected the Mediterranean sponge *Aplysina cavernicola* as a model species for this study. Actinide elements are not the only source of radioactive release in cases of civilian nuclear events, however their physico-chemo transfer mechanisms to marine species remain largely unknown. We have targeted europium(III) as a representative of the trivalent actinides such as americium or curium.

To unravel biological uptake mechanisms of europium in *Aplysina cavernicola* we have combined radiometric measurements (gamma) with spectroscopic (Time-Resolved Laser-Induced Fluorescence Spectroscopy, TRLIFS and X-ray Absorption Near Edge Structure, XANES) and imaging (Transmission Electron Microscopy, TEM and Scanning Transmission X-ray Microscopy, STXM) techniques.

We have observed that the colloids of $NaEu(CO_3)_2.nH_2O$ formed in seawater are taken up by *A. cavernicola* with no evidence that lethal dose has been reached in our working conditions. Spectroscopic results suggest that there is no change of speciation during uptake. Finally, TEM and STXM images recorded at different locations across a sponge crosssection, together with differential cell separation indicate the presence of europium particles (around 200 nm) mainly located in the skeleton and towards the outer surface of the sponge.

1. Introduction

In accidental situations involving nuclear reactors, noble gases and fission products as cesium or iodine contribute most significantly to the total radioactivity released. Although the actinide elements are generally not the major contributor to environmental radioactivity they can have long lasting impacts on human health and environment. Actinides are the only exogenous metals known to have no essential role in the normal biochemical processes occurring in living organisms. Unlike many other toxins, metals cannot be destroyed by living organisms – they can only be excreted. However, their speciation may change according to environment characteristics (e.g., pH, ionic strength), which can affect their bioavailability and toxicity. The chemical mechanisms leading to the specific binding of a metal to a given protein are particularly complex and a lack of specificity is often observed for the exogenous metals.[1] The actinides are chemical poisons as well as radiological hazards. Their chemical toxicity is thought to be similar to that of other heavy metals, while their radiotoxicity comes from high rates of alpha particle emission. Effects can be immediate or delayed for low doses, and depend on the intensity of the radiation, timescale and mechanism of the exposure, and the type of affected tissue. Knowledge of molecular actinide speciation in these biological environments is essential for impact assessment.

Seawater is likely to accumulate radionuclides regardless of whether the release occurs near a sea shore or further away, connected to the sea via rivers. Compared to many other environmental systems, seawater is perhaps one of the most complex systems because of its multivariate composition (anions, cations, organic matter), spatial heterogeneity (as a function of depth, for instance) and dynamic state (currents). The radionuclides may accumulate in soft tissue such as algae, which in turn could impact marine life and other organisms higher in the food chain.

The bioaccumulation of stable inorganic contaminants (often referred to as "heavy metals") has already been described in occurrence with organisms from all trophic levels such as algae, mussels, fish and sponges.[2-6] Among these organisms, sponges are immobile active filter feeders and have been identified as hyper accumulators of many heavy metals.[7-10] Several studies have shown that sponges are a good bioindicator of the presence of trace metals and for these reasons, sponges have been selected here as sentinel organisms for heavy elements in seawater. The Indian sponge *Spirastrella cuspidifera* accumulates, for example, cadmium, chromium and tin up to concentrations 5 to 7 orders of magnitude higher than in the bulk water.[8] The accumulation of metals is highly dependent on the species of sponge. Out of four Mediterranean species, only three (*Crambe crambe, Phorbas tenacior* and *Dysidea avara)* were shown to be copper bioindicators.[10] Although accumulation of elevated amounts of metals has been reported, relation to their specific physical chemical properties (e.g., oxidation state, hardness *vs*. softness) has rarely been described.[7-13] Therefore, it is essential to go beyond the phenomenological aspects of uptake and to describe accumulation chemical mechanisms.

We report in this paper on the accumulation mechanism of europium(III) in the Mediterranean sponge *Aplysina cavernicola*. Europium(III) was targeted for this study as a representative of the trivalent actinides such as americium or curium. Lanthanides are often taken as non-radioactive surrogates of the heavier actinide elements that are easier to manipulate, while retaining many of the same physico-chemical properties observed for actinides in the second half of the actinide series. Europium is commonly found in the +3 oxidation state and has relatively simple redox chemistry. In a previous work we have described the speciation of europium in seawater and the uptake behavior of americium at the ultra trace scale by *Aplysina cavernicola.*[14] Commonly found in the entrance of the caves off the coasts of the Northwestern Mediterranean, *Aplysina cavernicola*[15] was selected in this study as a model bioaccumulator. We have used in a unique manner the combination between gamma radiometry, spectroscopic and imaging probes to cast light on the uptake mechanism of europium. Thus, the following techniques have been employed: X-ray Absorption Near Edge Structure (XANES, L_{III} edge, $M_{IV,V}$ edges) as well as Time-Resolved Laser-Induced Fluorescence Spectroscopy (TRLIFS) for europium speciation in the sponge, Transmission Electron Microscopy (TEM) and Scanning Transmission X-ray Microscopy (STXM, at the Eu $M_{IV,V}$ edges) for europium localization. To our knowledge, this is one of the few attempts to combine uptake data with molecular structural data and imaging to explore the transfer mechanisms of heavy radionuclides (herein using europium as a surrogate) in a seawater organism.

2. Results and discussion

This section is divided in three parts: first the uptake behavior of *Aplysina cavernicola* for the europium element in doped seawater; second a comparison of europium speciation in seawater and after uptake in the sponge tissue; and lastly the localization of europium in sponge tissues.

2. 1. Europium bioaccumulation in *Aplysina cavernicola*

The accumulation curve of *A. cavernicola* for europium(III) with a cocktail of radiotracer ^{152}Eu and stable ^{151,153}Eu (see experimental section) has been recorded. Two sponges (sponges A and B) were exposed to a daily single dose of 30 Bq of ^{152}Eu together with 7.1 x 10^{-7} mol of stable Eu (corresponding to a total Eu concentration of 9.7 x 10^{-7} M (0.15 µg.ml^{-1}), for 15 h. At this concentration, the solubility limit of europium in seawater is reached (K_s around $10^{-17.5}$) and it was previously shown that its speciation is $NaEu(CO_3)_2.nH_2O$.[14] Nevertheless, no precipitate was observed during the experiment and a mixture of colloids and soluble phase must be present in solution as already discussed.[15]

Figure 1Sab (see supplementary materials) shows the water gamma measurements for sponges A and B (in Bq.g^{-1}) measured in water after injection of spike n and before injection of spike n+1. These measurements yielded an average uptake rate of *ca* 19 % for sponge A and 28 % for sponge B of Eu

transferred daily from the seawater to the sponge during the 15 hours exposure. Assuming that all the europium taken up by the sponge is not depurated from the sponge between exposures, the cumulated concentration of europium in the two sponges A and B after 11 exposures was estimated at 4.1 x 10^{-6} mol/g and 2.8 x 10^{-6} mol/g (normalized to sponge dry weight), respectively. Figure 1 shows the estimated accumulated total europium dose for both specimens. These estimated values are almost twice higher than the concentrations of europium directly measured by gamma spectrometry in the ground specimen at the end of the experiment, which were equal to 1.9 x 10^{-6} and 1.6 x 10^{-6} mol/g (normalized for dry weight) respectively. The difference observed may be due to a depuration of europium and/or to removal of residuals of europium present on the sponge surface during the rinsing before the analysis of the specimen. A concentration factor (ie ratio between the ^{152}Eu activity in the sponge (Bq/g) and its activity in seawater (Bq/g)) of 1630 and 2070 (± 20 %) was calculated in the sponge A and B, respectively. Concentration factors are species and biotope dependent,[16] and their comparison with other concentration factors obtained in natural or semi natural conditions is difficult since they are highly dependent on the chemical element itself, its speciation and concentration of the contaminant.[10, 11] For instance, in *A cavernicola* sponges, ultra-trace levels of americium have linear kinetics of accumulation,[14] similar to that represented in Figure 1 for europium. In this experiment, CFs with respect to dry weight were estimated around 830 and 1040 after 5 days accumulation. In summary, it can be asserted here that the europium complex present in seawater as colloidal forms of $NaEu(CO_3)_2.nH_2O$ is taken up by, and accumulated in the sponge. Among the two specimens tested in this study, none of them died during the 11-day experiment.

2. 2. Speciation of europium in *Aplysina cavernicola*

In the first step, global speciation was investigated on an entire sponge specimen, sponge C, which was only contaminated with stable europium (at a similar concentration introduced into the water per spike), with a resulting concentration factor comparable to sponges A and B: 910 ± 270. A combination of TRLIFS and XANES spectroscopy at Eu L_{III} edge was implemented. Eu L_{III} edge Extended X-ray Absorption Fine Structure (EXAFS) was impossible to record because of the presence of iron in the sponge at about the same level as europium (the Fe K edge and Eu L_{III} edge absorptions occur at similar energies), and attempts at Eu K edge EXAFS measurements provided data with a signal to noise ratio that precluded interpretation.

The TRLIFS spectrum of sponge C contaminated with stable europium is presented in Figure 2. Europium has a characteristic luminescence spectrum in the red which makes it an ideal element for TRLIFS with its strongest lines around 580, 593, 617, 650 and 700 nm ($^5D_0 \rightarrow {}^7F_J$ J= 0 – 4) [17, 18]. The main fluorescent wavelengths used are at 593 nm and the hypersensitive ($^5D_0 \rightarrow {}^7F_2$) at 617 nm together with 580 nm. Characteristic shifts in the peak maxima and intensities of the hypersensitive band change significantly upon coordination [17, 19]. The spectrum presents two peaks at 593 and 616

159 nm. As expected, in the contaminated sponge, the intensity of the hypersensitive band is enhanced
160 relative to a spectrum of europium in dilute aqueous $HClO_4$ (aquo form of Eu) which is an indication
161 of complexation (Figure 2). Moreover, the spectrum shows a large contribution between 500 and 600
162 nm which is characteristic of marine organic matter[20] or more likely to sponge itself (it was not
163 possible to eliminate this luminescence by time resolution). The peak ratio I_{593}:I_{616} obtained after
164 spectral deconvolution is 1:3 and the luminescence lifetime is 200 ± 60 µs (different from the lifetime
165 of aquo Eu equal to 110 +/- 10 µs). This peak ratio suggests the presence of a majority of biscarbonate
166 species, $Eu(CO_3)_2^-$ as in seawater.[17, 18, 21]
167 The lifetime is of the same order as that measured in a previous study for $NaEu(CO_3)_2.nH_2O$ (between
168 100 and 150 µs[14]) in a colloidal solution. As observed in Figure 2, even when using time resolution,
169 the contribution of the sponge background is important at this level of europium concentration and
170 data analysis is difficult. However, the TRLIFS measurement strongly suggests that europium
171 speciation is similar in seawater and in the sponge. It should finally be noted that in the environment
172 around pH 8, carbonate species are major species. However, as shown previously by speciation
173 modelling, the formation of hydroxides or hydroxocarbonates is also possible, although in proportions
174 of less than 20% [14]. In any case it has not be observed here since only one lifetime was measured.
175 To confirm this hypothesis, the europium speciation in the sponge was probed by XANES at the
176 europium L_{III} edge. It has already been shown that lanthanide L_{III} edge can be sensitive to structural
177 information[22]. P. d'Angelo et al. have used XANES spectra at the L_{III} edge to obtain information on
178 the geometric structure of hydration clusters, especially for the lighter lanthanides[22]. Figure 3 shows
179 the derivative of the XANES spectra normalized in absorption intensity and in energy compared with
180 the spectra of europium in seawater ([Eu] = 5x10-5 M)[15]. This comparison clearly supports the
181 interpretation given above that the speciation of Eu in the sponge and seawater is comparable and
182 resembles carbonate compounds. This confirms the TRLIFS analysis and suggests that europium is
183 present within the sponge with the same speciation as in seawater.
184
185 **2. 3. Localization of europium in *Aplysina cavernicola***
186
187 To further explore the europium interaction with the sponge and its transfer mechanisms,
188 localization investigations were performed with a combination of X-ray and electron microscopy.
189 Sponge slices were prepared at two characteristic locations as shown in Figure 4: near the osculum (1)
190 and near the external surface (2). These locations were chosen specifically to estimate the distribution
191 of europium in the sponge, given that differences were expected if the cation were to pass through the
192 sponge or if it were only adsorbed on the surface.
193 Representative data obtained by STXM at 1128 eV (europium M_V edge) for the two different
194 regions are shown in Figure 5. It shows several large, higher-contrast objects around 10 µm sizes that
195 correspond to the spherulous cells of the sponge. The role of these cells is not precisely defined

196 although they have been reported to assist in waste disposal mechanisms for the sponge.[23] Rather than
197 finding a homogenous distribution, europium was localized as distinct particles (outlined by black
198 circles in Figure 5) found in skeleton areas outside the spherulous cells in both region (1) and (2). The
199 europium particles were roughly 100 - 200 nm in diameter (Figure 6a) and were observed everywhere
200 in the sponge. The presence of these distinct particles suggests that europium does not form soluble
201 complexes. A XANES spectrum was also measured on the particle shown in Figure 6b at the
202 europium $M_{IV,V}$ edges (1159 and 1128 eV respectively).[24] It is further compared in Figure 6b to the
203 spectrum of a particle obtained directly from seawater (see experimental section). Both spectra are
204 indistinguishable within the sensitivity limits of Eu $M_{IV,V}$ XANES. Similar particles were also
205 observed by TEM as shown in Figure 7 in location (1). Although TEM has better spatial resolution,
206 particles with the same size as observed by STXM were observed on the skeleton. This description of
207 the speciation is confirmed by previous observations by TRLIFS and XANES and suggests that
208 precipitation of the colloids present in seawater occurs in the sponge tissues as the main mechanism.
209 To further confirm that europium particles were mainly located in the skeleton, cell separation was
210 performed by differential centrifugation on the sponges A and B, which were contaminated with ^{152}Eu
211 and stable ^{151,153}Eu, respectively.[25-28] This procedure resulted in isolation of three fractions: the
212 skeleton fraction together with spherulous cells, a sponge cell fraction, and a bacterial fraction. Since
213 it is difficult to achieve a perfect separation of the sponge cells without causing significant damage, it
214 was only possible to measure each fraction by gamma spectrometry in a semi-qualitative manner.
215 Figure 8 shows that 80% of the europium activity is located in the first fraction (skeleton and
216 spherulous cells fraction). Remembering that STXM images suggested (although qualitatively) that
217 europium was not interacting with the spherulous cell, this confirms a major localization in the
218 skeleton. Nonetheless, a significant amount of europium (below 20%) was found in the cell fraction.
219 Indeed, clusters of those europium particles were also observed in a vacuole of about 300 to 600 nm as
220 shown by the TEM image of Figure 9. In summary, the combination of STXM, TEM and differential
221 cell separation indicates the presence of europium mainly in the skeleton at the outer surface of the
222 sponge around location (2). Previous studies have shown that *Aplysina cavernicola* possesses a three-
223 dimensional skeleton. This fibrous skeleton is composed of spongin-based and chitin fibers [29]. It is
224 known that chitin has a high ability to sorb heavy metals as actinides [30]. Likewise, some studies have
225 revealed that spongin fibers concentrate metals such as iron and lead [10]. However in the present study
226 no evidence of europium complexation with a part of the fibrous skeleton has been observed. This
227 suggests, together with the speciation analysis that europium colloids are transferred from the seawater
228 medium through the sponge surface *via* the pores present on the external walls. Nonetheless, the
229 presence of similar particles at lower concentrations was also detected in all parts of the sponge and
230 near the osculum.
231

In conclusion, knowledge of chemical speciation for impact assessments on living organisms is crucial not only in regard to concentration or dose but to physico-chemical parameters as well. In this report, we have developed a case study to unravel the accumulation mechanisms of europium in marine organisms. Among them, sponges are immobile active filter feeders and have already been identified as hyper accumulators of several heavy metals but the chemical mechanisms of accumulation have never been determined. In this study europium was taken as a chemical surrogate of heavy actinide oxidation state +III and the selected sponge species is the Mediterranean sponge *A. cavernicola*. To our knowledge, this is one of the few attempts to combine uptake data with spectroscopic and imaging data to explore the transfer mechanisms of actinides (here using the europium surrogate) in a seawater organism.

In the first part, the uptake curve of sponge *A. cavernicola* with a cocktail of radiotracer ^{152}Eu and stable ^{151,153}Eu in seawater was recorded, reaching concentration factors between 1600 and 2100. Among the two specimens tested in this study, none of them died during the 11-day experiment indicating that no lethal dose has been reached in our working conditions (0.15 $\mu g.ml^{-1}$ per spike over 187 hours). In conclusion, the colloids of $NaEu(CO_3)_2.nH_2O$ formed in seawater under the current conditions are taken up by *A. cavernicola* with no evidence of mortality for the specimen tested in our conditions. In the second part, the global speciation of europium within the sponge was investigated using both TRLIFS and XANES (Eu L_{III} edge) probes. Both probes are specific for europium speciation. In both cases, the spectroscopic data suggests that the europium speciation inside the sponge may be described as a carbonate complex comparable to that already observed in seawater near the europium solubility limit (K_s around $10^{-17.5}$). This suggests that there is no modification of the speciation during sponge uptake. Finally, in the third part, the localization of europium inside the sponge compartments was performed with a combination of STXM and TEM. Images recorded at two different locations on a sponge cross section, together with differential cell separation indicate the presence of europium particles (around 200 nm) mainly located in the skeleton and mainly towards the outer surface of the sponge. The $M_{IV,V}$ XANES spectrum of a particle confirms the above speciation. This observation together with the speciation analysis suggests that europium colloids present in seawater as $NaEu(CO_3)_2.nH_2O$ are transferred from the seawater medium through the sponge surface *via* the surface pores in the vicinity of which they are precipitated as particles of a few hundred nm. Nonetheless more complex uptake mechanisms may also occur, although in a minor percentage, since the presence of similar particles was also detected in cell vacuoles far from the surface. This study goes beyond the field of environmental radiochemistry and illustrates how important it is to specify speciation to unravel accumulation mechanisms in living organisms in general.

3. Experimental

3. 1. Europium bioaccumulation

Three specimens of the Mediterranean sponge *Aplysina cavernicola*, a tubular yellow sponge with spongin and chitin fibers, were collected by Self-Contained Underwater Breathing apparatus (SCUBA) diving at a 25 m depth in the entrance of a cave off the coast of Saint-Jean-Cap-Ferrat (France, 43° 41′ 29″ N, 7° 19′ 11″ E). Individuals of homogeneous size, with an average length close to 3.0 cm and an average diameter of 1.4 cm, were selected.

Two accumulation experiments were performed: one with both ^{152}Eu (for tracing) and natural europium (sponges A and B), to follow the accumulation in the sponge and to evaluate its dispersion in the sponge, and the other with only natural europium (sponge C), in order to perform EXAFS and STXM measurements.

A stock solution of ^{152}Eu radiotracer (4.49 kBq/g in 0.1 N HCl) was obtained by diluting a solution of $EuCl_3$ (LEA, Eu152ELSB30, 40 kBq/g) in 0.1 N HCl. The stock solution of natural ^{151,153}Eu (0.071 mmol, 10.8 mg/ml) was prepared by dissolving $Eu(NO_3)_3.6H_2O$ (Prolabo, purity > 99 %) in 0.1 N HCl. Before the uptake experiments, specimens were acclimated for a few days in a 20 l aquarium. For the uptake measurements, a contamination cycle was performed every day according to the following procedure: for 9 h, sponges A and B were maintained in an open water system; then, the sponges were placed in 735 ml boxes in the same aquarium, and maintained in a closed water system. The radiotracer and the natural europium were spiked by the addition of 10 µl of each stock solution in the seawater corresponding to an activity of 30 Bq in ^{152}Eu and an amount of 7.10^{-7} mol of ^{151,153}Eu per spike. After 15 hours exposure, the system was opened for sponge recovery. This cycle was repeated 11 times. In order to assess potential americium adsorption on the boxes, a blank test consisting of spiking an empty 735 ml box was performed. The blank test revealed that less than 0.5 Bq were adsorbed on the plastic boxes during the entire procedure. The uptake curve was obtained using gamma radiometry. At the end of each 15 h spike sequence, 50 ml of seawater were taken off the 735 ml box and the associated gamma activity was measured by gamma spectrometry. The difference between the spiked activity (measured after spike n in Figure 1Sab) and the measured activity after the 15 h spike sequence (measured before spike n+1 in Figure 1Sab) indicated potential uptake by the sponge

$$[\mathrm{Eu}]\ (\mathrm{in\ g.mol^{-1}}) = \frac{1}{A(152\mathrm{Eu}).\mathrm{M}_{152}}\{\mathrm{A(after\ spike(n))} - \mathrm{A(before\ spike(n+1))}\} \times \frac{1}{R_{152/151,153}}$$

with $A(^{152}\mathrm{Eu})$ = massic activity of Eu ($6.45.\ 10^{12}$ Bq.g^{-1}), M_{152} is the molar mass of Eu and $R_{152/151,153}$ the ratio between ^{152}Eu and ^{151,153}Eu in the spike.

At the end of the experiment, the sponges were collected and rinsed in clean seawater to remove radiolabeled water.

Gamma-ray measurements of the samples were carried out with a high resolution γ spectrometer with a coaxial high purity germanium (HPGe) detector (ORTEC GEM 100 - 95) in a shielded environment with graded castle, 10 cm lead and 0.5 cm thick copper. The gamma emission of ^{152}Eu was assayed at

122 and 344 keV. The efficiencies were respectively of 0.086 +/-0.005 and 0.063+/-0.004. Counting time was adjusted to obtain counting errors below 10%.

The sponge C exposure procedure for the EXAFS and STXM measurements, was similar than that used for the sponges A and B with the exception that only the natural europium ^{151,153}Eu was added to the seawater.

3. 2. TRLIFS

A Nd-YAG laser (Model Surelite Quantel) operating at 355 nm (tripled) and delivering about 10 mJ of energy in a 10 ns pulse with a repetition rate of 10 Hz, was used as the excitation source for europium. The laser output energy was monitored by a laser power meter (Scientech). The focused output beam was directed into the 0.35 µl quartz cell for solid samples of the spectrofluorometer (F900-Edinburgh). The detection was performed by an intensified charge coupled device (Andor Technology) cooled by Peltier effect (-5°C) and positioned at the polychromator exit for the emission spectra measurement and by a photomultiplier tube (PMT) to measure fluorescence decay time. Logic circuits, synchronized with the laser shot beam, allowed the intensifier to be activated with determined time delay (from 0.005 to 1000 µs) and during a determined aperture time (from 0.005 to 1000 µs). From a spectroscopic point of view, various gate delay and duration were used to certify the presence of only one complex by the measurement of a single fluorescence lifetime and spectrum. The fluorescence spectra and fluorescence decay curves were accumulated 1000 times and analyzed using the software ORIGIN 8.0. All peaks were described using a mixed Gaussian-Lorentzian profile. Fluorescence lifetime measurements were made by varying the temporal delay with fixed gate width.

3. 3. XANES

X-ray absorption experiments at the Eu L_{III} edge were carried out on the MARS beamline of the SOLEIL synchrotron facility.[31, 32] The optics of the beamline essentially consist of a water-cooled double-crystal monochromator (FMB Oxford), which is used to select the incident energy of the X-ray beam and for horizontal focalization, and two large water-cooled reflecting mirrors (IRELEC/SESO) that are used for high-energy rejection (harmonic part) and vertical collimation and focalization. In this case, the monochromator was set with the Si(111) crystals and the mirrors with the Si strips. Energy calibration was performed at the Fe K edge at 7112 eV. XANES measurements were performed in fluorescence mode, due to the low concentration, using a 13-element high purity germanium detector (ORTEC). Data processing was carried out using the Athena code.[33] The e_o energy was identified at the maximum of the absorption edge. XANES scans were taken from 6850 to 7010 eV with a 0.5 eV step. Data were collected at 3 seconds per step, and the integrated fluorescence was normalized. The experimental XANES spectrum of contaminated sponge was compared to XANES spectrum of europium doped seawater at 5 x 10^{-5} M.[14]

3. 4. STXM

STXM methodology was similar to that discussed previously.[34, 35] X-ray microscopic images were obtained with a STXM at the Advanced Light Source, at the Molecular Environmental Science beamline 11.0.2 (ALS-MES, Lawrence Berkeley National Laboratory, U.S.A.). Energy calibrations were performed at the Ne K-edge for Ne (867.3 eV). In our experiments, a microtome was used to create 1 μm thick slices of sponge (specimen C), which were placed on a 100 nm thick silicon nitride window (1 mm square). Particles from seawater were centrifuged from a seawater doped solution with [Eu] = 5 10^{-5} M.[18] For these measurements, the X-ray beam was focused with a zone plate onto the sample, and the transmitted X-rays were detected. Images at a single energy were obtained by raster-scanning the sample and collecting X-rays as a function of sample position. Spectra at each image pixel or particular regions of interest on the sample image were extracted from the "stack," which is a collection of images recorded at multiple, closely spaced photon energies across the absorption edge. Data treatment was performed with aXis2000 code developed at McMaster University.[36] NEXAFS spectra at the Eu $M_{V,IV}$ edges were recorded from stack images and normalized (intensity and energy) with respect to the most intense M_V peak at 1130.6 eV. During the STXM experiment, particles showed no sign of radiation damage, and each spectrum was reproduced several times on independent particles and different samples.

3. 5. Partition studies

Sponge tissue (sponges A and B) was carefully rinsed with CMF-ASW, pH 7.4, to remove seawater and then chopped into small pieces and placed with a minimum volume of CMF-ASW with glutaraldehyde (3%). The solution was then filtered through nylon mesh (50 μm size). The resulting cell suspension was spun first at 200 g and 4°C for 5 min. The pellet was washed twice with fresh CMF-ASW (fraction 1) and is composed of the skeleton and spherulous cells. The supernatant was then spun at 600 g at 4° C for 5 min allowing to isolate fraction 2 with the sponge cells. After rinsing, the supernatant was spun at 4500 g and 4°C for 15 min. This last fraction (fraction 3) is composed of bacteria.

Acknowledgements

This work was jointly financed by the DPN (Direction of Nuclear Propulsion) CEA/DAM and CNRS / Institut National de Chimie. The experimental work using sponges was conducted under an internship at the IAEA-Environment Laboratories in Monaco. The International Atomic Energy Agency is grateful to the Government of the Principality of Monaco for the support provided to its Environment Laboratories. XAS experiments were performed at the MARS beam line of SOLEIL synchrotron, Gif

sur Yvette, France. The authors wish to thank Pr O. P. Thomas and M. A. Tribalat for providing the sponge specimens and S. Pagnotta from the Microscopy Service (UNS) for TEM analysis. D. K. Shuh, S. G. Minasian are supported by the Director, Office of Science, Office of Basic Energy Sciences, Division of Chemical Sciences, Geosciences, and Biosciences Heavy Element Chemistry Program of the U.S. DOE at LBNL under Contract No. DE-AC02-05CH11231. The ALS and TT were supported by the Director, Office of Science, Office of Basic Energy Sciences, of the U.S. DOE under Contract No. DE-AC02-05CH11231 at LBNL. Research at Beamline 11.0.2 at the ALS was supported by the Director, Office of Science, Office of Basic Energy Sciences, Division of Chemical Sciences, Geosciences, and Biosciences Condensed Phase and Interfacial Molecular Sciences Program of the U.S. DOE at LBNL under Contract No. DE-AC02-05CH11231.

392

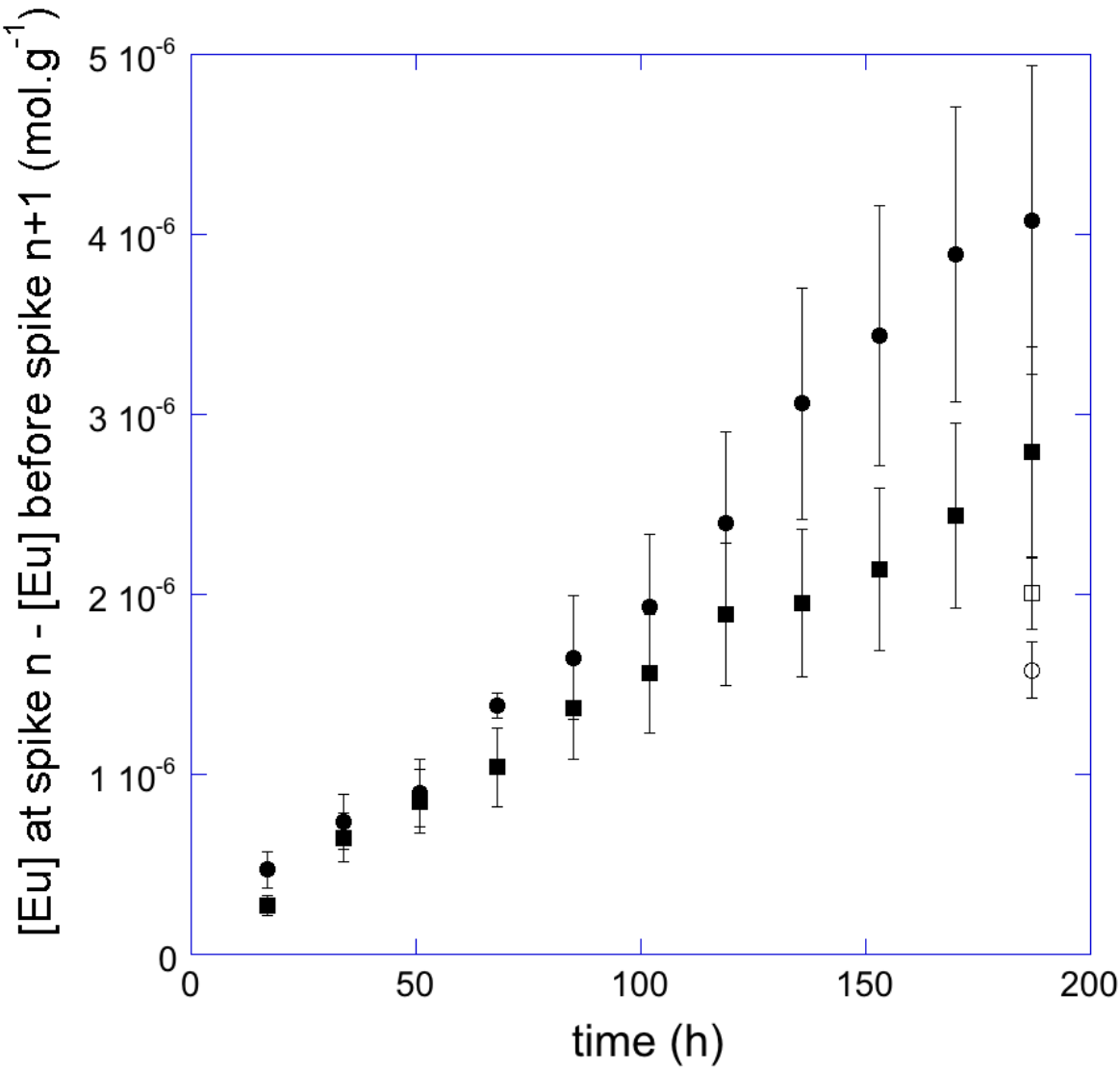

393

394

395 Figure 1: Concentration of ^{152}Eu europium in two *A. cavernicola* sponges after daily exposure to a
396 cocktail of ^{152}Eu and ^{151,153}Eu as explained in the experimental section. Estimated cumulated europium
397 concentrations (A, ● and B, ■) are calculated from gamma measurements, assuming that none of the
398 europium taken up is excreted out of the sponge between each exposure. Measured concentration of
399 europium in the sponge at the end of the experiment (A, ○ and B, □) are also reported. The total
400 amount introduced in seawater at the end of the experiment is equal to [Eu] = 1.76 x 10^{-5} mol.g^{-1}.

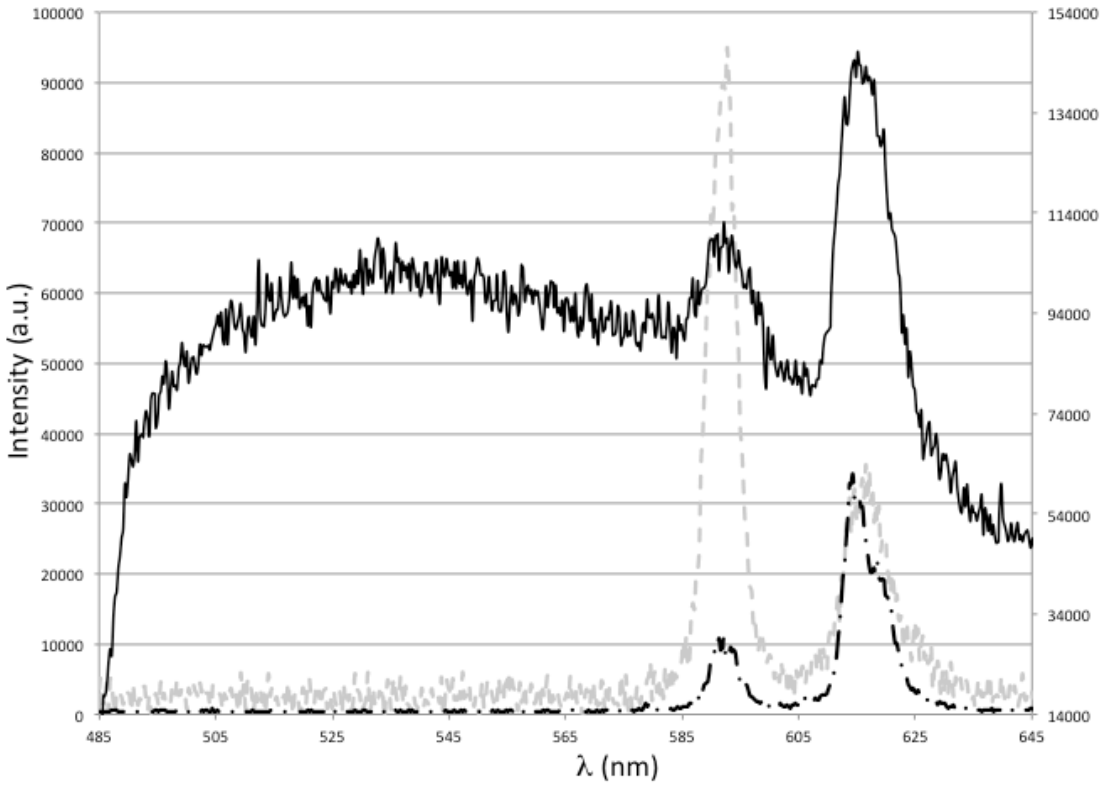

Figure 2: TRLIFS spectra of contaminated sponge (speciment C) with europium (black plain curve), europium in doped seawater at [Eu] = 5.10^{-5} M (black dotted curve[14]) and free europium in $HClO_4$ 0.1 M (grey dotted curve[18]). Time delay 5 µs, aperture time 600 µs, number of accumulations 1000.

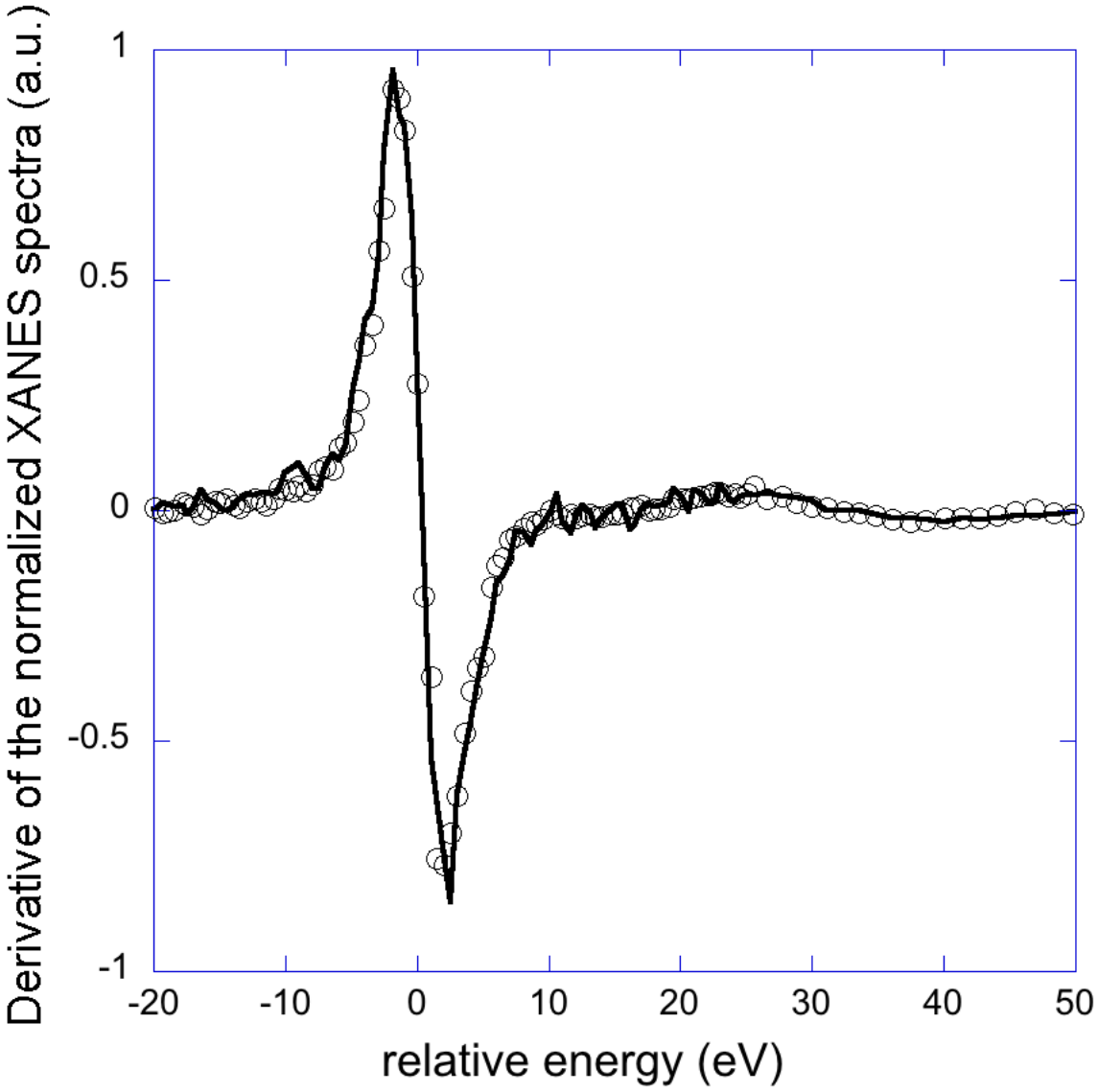

Figure 3: Derivative of the normalized L_{III} edge XANES spectra of Eu in seawater (normalization has been performed on the XANES spectra with an absorption edge of 1). Eu in seawater with [Eu] = 5 x 10^{-5} M (○); in sponge C (solid line). For clarity, the abscises have been normalized to zero at the edge inflection point.

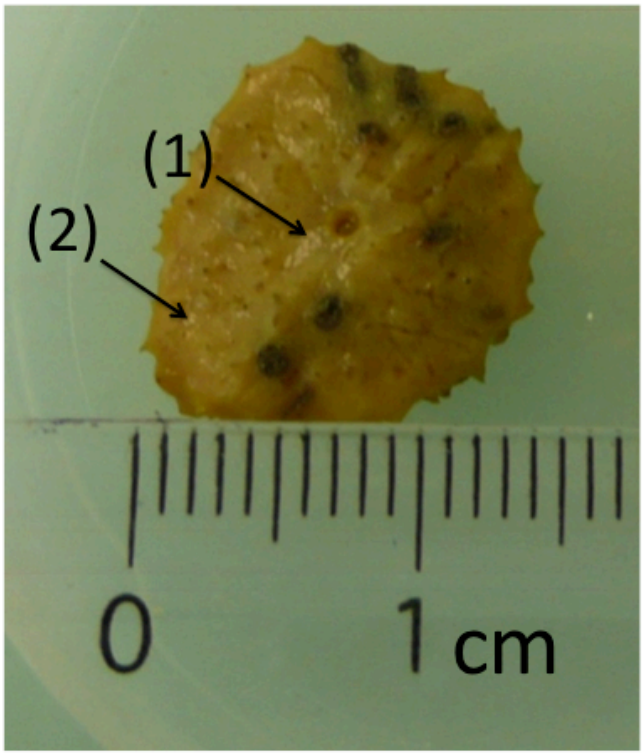

Figure 4: Localization of the two different cross section areas on *A. cavernicola* (specimen C) for STXM measurements: near the osculum (arrow (1)), and near the outer edge (arrow (2)).

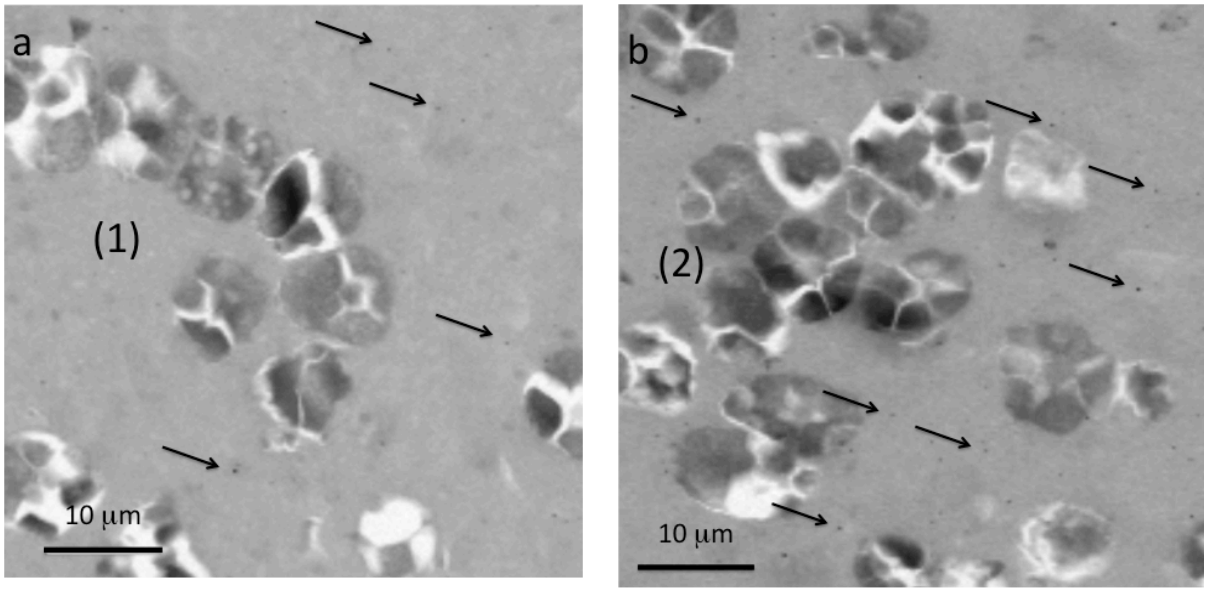

Figure 5: STXM contrast images at 1132 eV of the sponge contaminated with europium (a) near the osculum in region (1) and (b) near the external surface in region (2). Some of the europium particles are outlined by arrows and should not be regarded as a precise accounting of all particles.

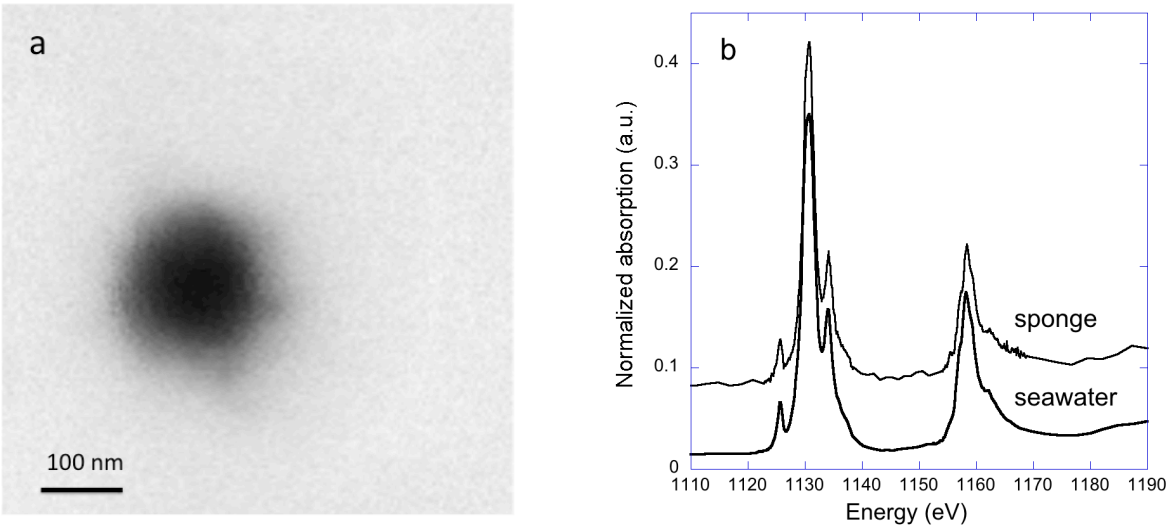

Figure 6: (a) STXM images in location (1): An europium colloid in contaminated sponge C; (b) $M_{IV,V}$ edge XAS obtained from the particle compared with data obtained from Eu in seawater (see experimental section). Normalization has been performed on the peak at 1130.6 eV.

435

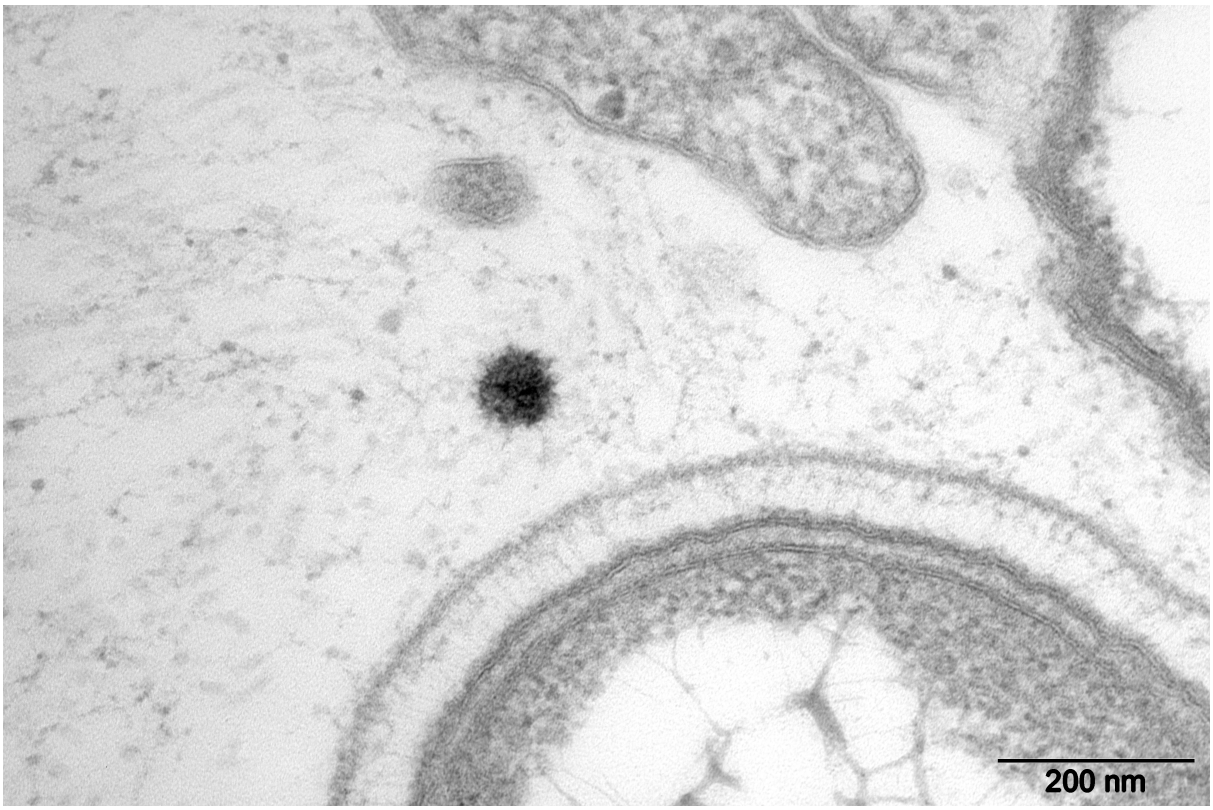

436
437
438 Figure 7: TEM image in location (1): A europium particle located in the skeleton in contaminated
439 sponge C.
440

441

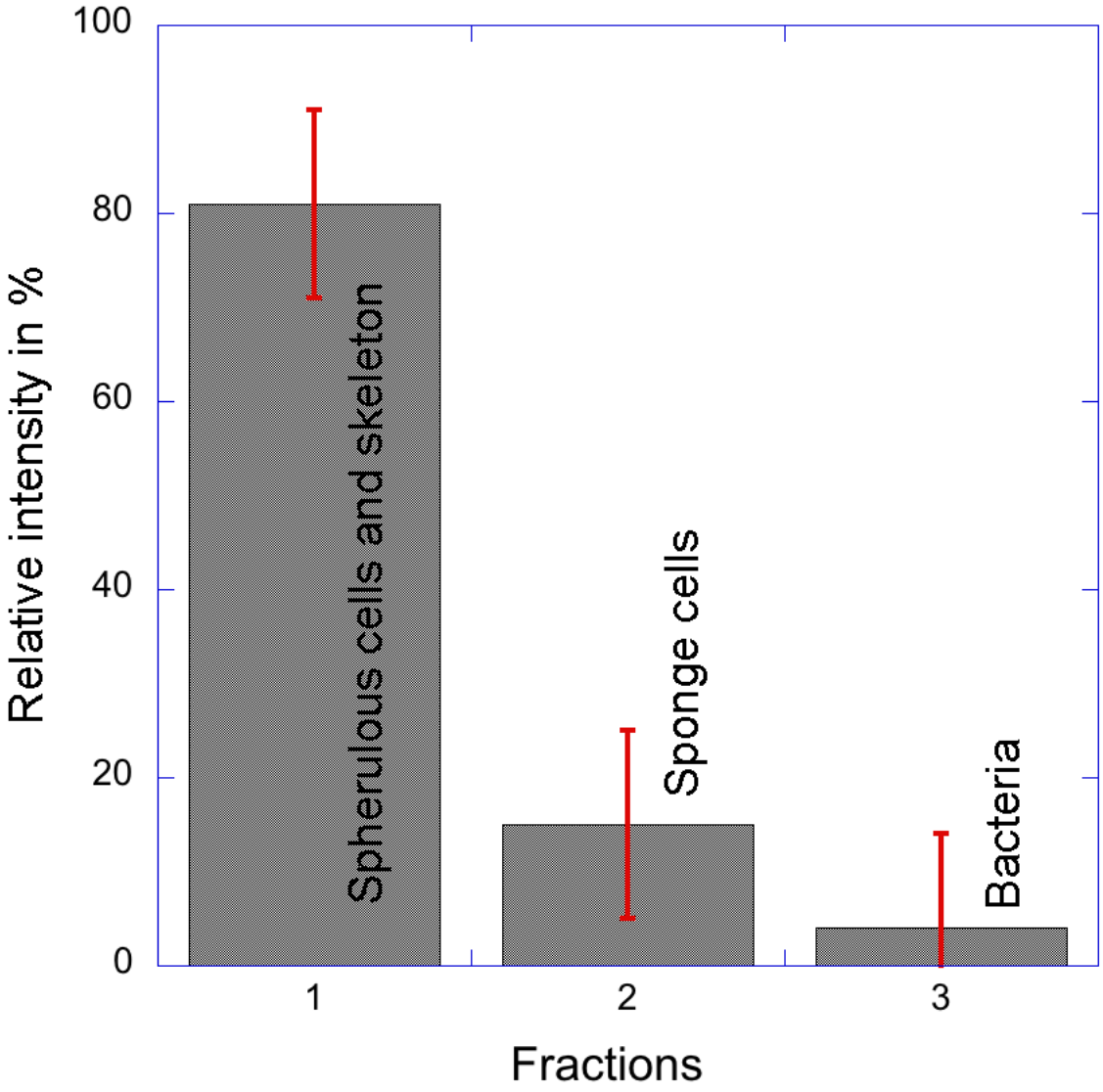

442
443
444 Figure 8: Qualitative indication of the ^{152}Eu activity present in the different fractions (skeleton, cells
445 and bacteria) after separation by gradient centrifugation of contaminated sponges A and B.

446

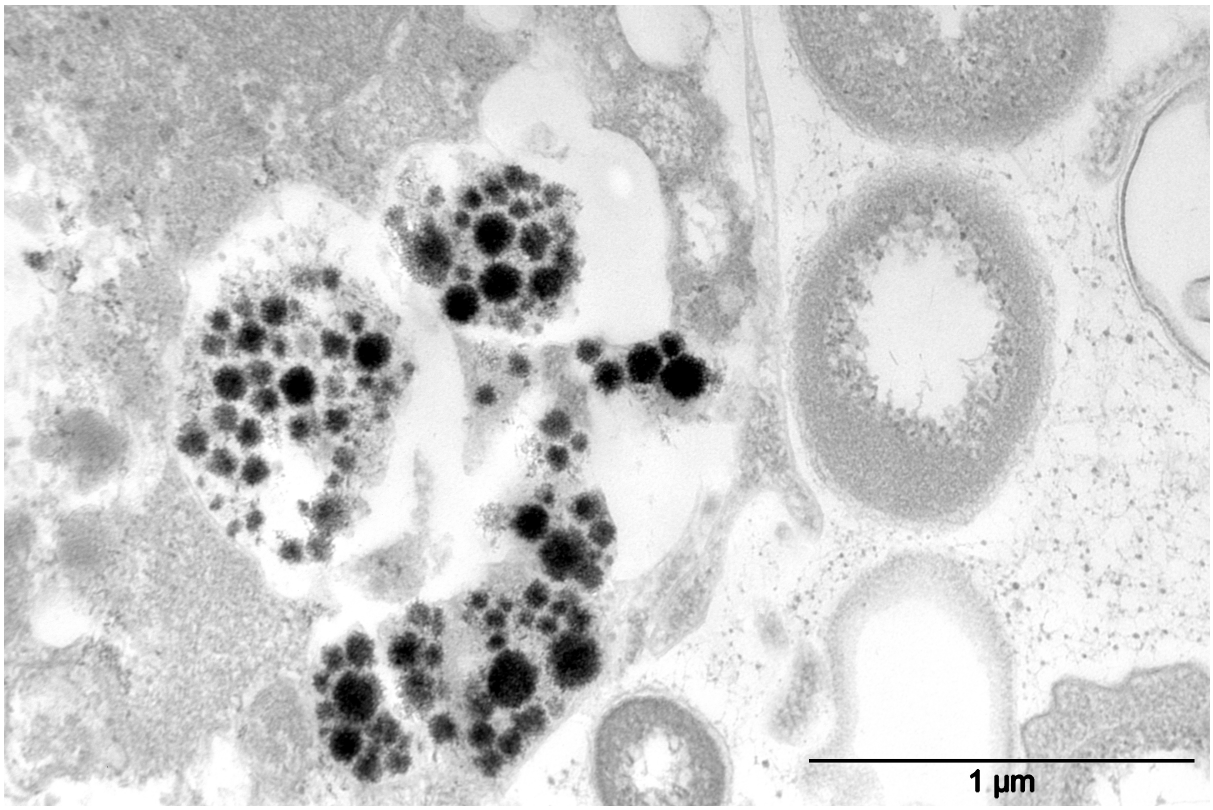

Figure 9: TEM images of a cluster of europium colloids contained in a cell vacuole of contaminated sponge C.

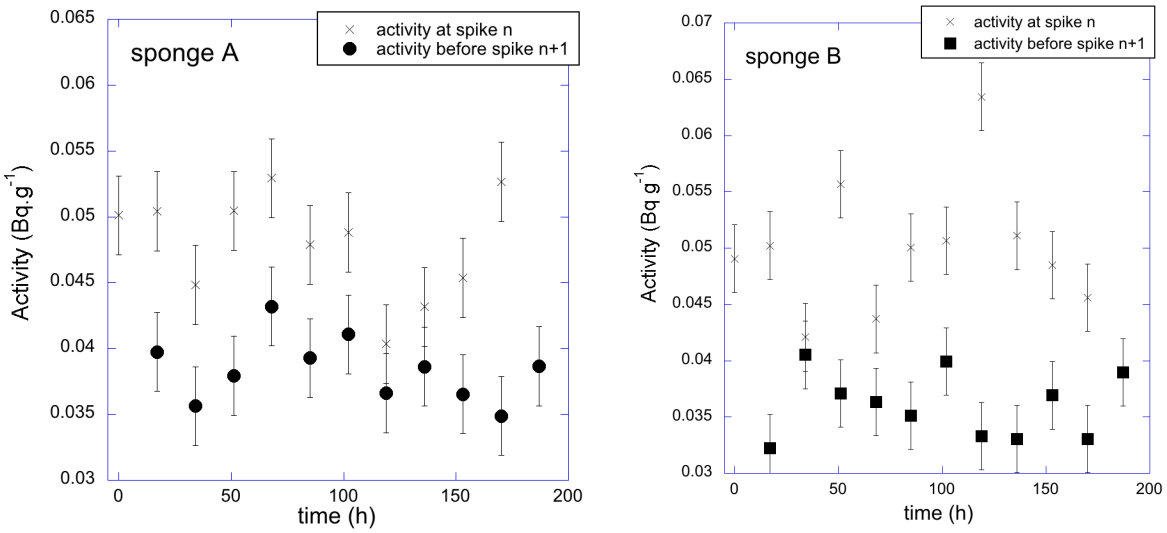

455 Figure 1Sab: Gamma activity measured in seawater after each spike n (initial concentration) and just
456 before spike n+1 (corresponding to the sponge uptake) for sponges A and B.

457
458

459 Graphical TOC

460

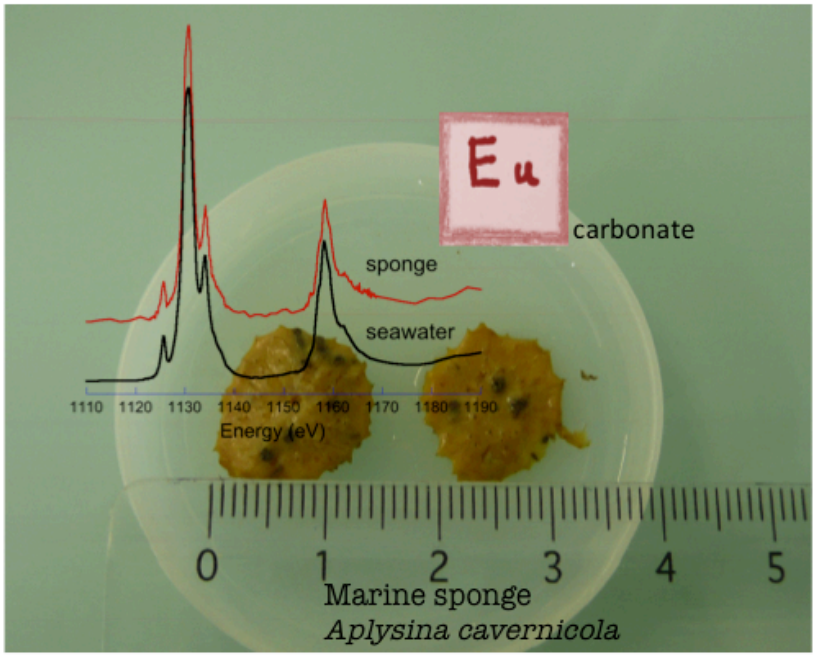

461

462

463

464 **References**

465

466 1. Wang, S.; Shi, X., Molecular mechanisms of metal toxicity and carcinogenesis. *Molecular and*
467 *cellular biochemistry* **2001,** *222*, (1-2), 3-9.
468 2. Neff, J. M., *Bioaccumulation in marine organisms: effect of contaminants from oil well*
469 *produced water*. Elsevier: **2002**.
470 3. Mason, R.; Laporte, J.-M.; Andres, S., Factors controlling the bioaccumulation of mercury,
471 methylmercury, arsenic, selenium, and cadmium by freshwater invertebrates and fish. *Archives of*
472 *Environmental Contamination and Toxicology* **2000,** *38*, (3), 283-297.
473 4. Boening, D. W., An evaluation of bivalves as biomonitors of heavy metals pollution in marine
474 waters. *Environmental monitoring and assessment* **1999,** *55*, (3), 459-470.
475 5. Nelson, W. G.; Bergen, B. J.; Cobb, D. J., Comparison of PCB and trace metal
476 bioaccumulation in the blue mussel, Mytilus edulis, and the ribbed mussel, Modiolus demissus, in new
477 Bedford Harbor, Massachusetts. *Environmental toxicology and chemistry* **1995,** *14*, (3), 513-521.
478 6. Roditi, H. A.; Fisher, N. S.; Sañudo-Wilhelmy, S. A., Field testing a metal bioaccumulation
479 model for zebra mussels. *Environmental science & technology* **2000,** *34*, (13), 2817-2825.
480 7. Genta-Jouve, G.; Cachet, N.; Oberhaensli, F.; Noyer, C.; Teyssié, J.-L.; Thomas, O. P.;
481 Lacoue-Labarthe, T., Comparative bioaccumulation kinetics of trace elements in Mediterranean
482 marine sponges. *Chemosphere* **2012,** *89*, 340-349.
483 8. Patel, B.; Balani, M.; Patel, S., Sponge 'sentinel'of heavy metals. *Science of the total*
484 *environment* **1985,** *41*, (2), 143-152.
485 9. De Mestre, C.; Maher, W.; Roberts, D.; Broad, A.; Krikowa, F.; Davis, A. R., Sponges as
486 sentinels: patterns of spatial and intra-individual variation in trace metal concentration. *Marine*
487 *Pollution Bulletin* **2012,** *64*, (1), 80-9.
488 10. Cebrian, E.; Uriz, M. J.; Turon, X., Sponges as biomonitors of heavy metals in spatial and
489 temporal surveys in northwestern Mediterranean: multispecies comparison. *Environmental Toxicology*
490 *and Chemistry* **2007,** *26*, (11), 2430-2439.
491 11. Cebrian, E.; Agell, G.; Marti, R.; Uriz, M. J., Response of the Mediterranean sponge
492 Chondrosia reniformis Nardo to copper pollution. *Environ Pollut* **2006,** *141*, (3), 452-8.
493 12. Cebrian, E.; Martí, R.; Uriz, J. M.; Turon, X., Sublethal effects of contamination on the
494 Mediterranean sponge Crambe crambe: metal accumulation and biological responses. *Marine*
495 *Pollution Bulletin* **2003,** *46*, (10), 1273-1284.
496 13. Cebrian, E.; Uriz, M. J., Contrasting effects of heavy metals on sponge cell behavior. *Arch*
497 *Environ Contam Toxicol* **2007,** *53*, (4), 552-8.
498 14. Maloubier, M.; Michel, H.; Solari, P. L.; Moisy, P.; Tribalat, M. A.; Oberhaensli, F. R.;
499 Dechraoui Bottein, M. Y.; Thomas, O. P.; Monfort, M.; Moulin, C.; Den Auwer, C., Speciation of

americium in seawater and accumulation in the marine sponge Aplysina cavernicola. *Dalton Trans* **2015,** *44*, (47), 20584-96.

15. Vacelet, J. Répartition générale des éponges et systématique des éponges cornées de la région de Marseille et de quelques stations méditérrannéennes. **1959**.

16. IAEA *Handbook of parameter values for the prediction of radionuclide transfer to wildlife*; Technical Report Series n°479; International Atomic Energy Agency Vienna, **2014**.

17. Plancque, G.; Moulin, V.; Toulhoat, P.; Moulin, C., Europium speciation by time-resolved laser-induced fluorescence. *Analytica Chimica Acta* **2003,** *478*, (1), 11-22.

18. Moulin, C.; Wei, J.; Iseghem, P. V.; Laszak, I.; Plancque, G.; Moulin, V. r., Europium complexes investigations in natural waters by time-resolved laser-induced fluorescence. *Analytica Chimica Acta* **1999,** *396*, (2-3), 253-261.

19. Binnemans, K., Interpretation of europium(III) spectra. *Coordination Chemistry Reviews* **2015,** *295*, 1-45.

20. Clark, C. D.; Jimenez-Morais, J.; Jones Ii, G.; Zanardi-Lamardo, E.; Moore, C. A.; Zika, R. G., A time-resolved fluorescence study of dissolved organic matter in a riverine to marine transition zone. *Marine Chemistry* **2002,** *78*, (2-3), 121-135.

21. Kimura, T.; Kato, Y., Luminescence study on hydration states of lanthanide (III)–polyaminopolycarboxylate complexes in aqueous solution. *Journal of alloys and compounds* **1998,** *275*, 806-810.

22. D'Angelo, P.; Zitolo, A.; Migliorati, V.; Mancini, G.; Persson, I.; Chillemi, G., Structural Investigation of Lanthanoid Coordination: a Combined XANES and Molecular Dynamics Study. *Inorganic Chemistry* **2009,** *48*, (21), 10239-10248.

23. Vacelet, J., Les cellules à inclusions de l'éponge cornée verongia cavernicola vacelet. *J Microscopie* **1967,** *6*, 237-240.

24. Ruck, B.; Trodahl, H.; Richter, J.; Cezar, J.; Wilhelm, F.; Rogalev, A.; Antonov, V.; Do Le, B.; Meyer, C., Magnetic state of EuN: X-ray magnetic circular dichroism at the Eu $M_{4,5}$ and $L_{2,3}$ absorption edges. *Physical Review B* **2011,** *83*, (17), 174404.

25. Flowers, A. E.; Garson, M. J.; Webb, R. I.; Dumdei, E. J.; Charan, R. D., Cellular origin of chlorinated diketopiperazines in the dictyoceratid sponge Dysidea herbacea (Keller). *Cell and Tissue Research* **1998,** *292*, 597 - 607.

26. Song, Y.-F.; Qu, Y.; Cao, X.-P.; Zhang, W., Cellular localization of debromohymenialdisine and hymenialdisine in the marine sponge Axinelle sp. using a newly developed cell purification protocol. *Marine Biotechnology* **2011**, *13*, 868-882

27. Bewley, C. A.; Holland, N. D.; Faulkner, D. J., Two classes of metabolites from Theonella swinhoei are localized in distinct populations of bacterial symbionts. *Experientia* **1996,** *52*, 716 -722.

28. Garson, M. J.; Flowers, A. E.; Webb, R. I.; Charan, R. D.; McCaffrey, E. J., A sponge / dinoflagellate association in the haplosclerid sponge Haliclona sp. : cellular origin of cytotoxic alkaloids by Percoll density gradient fracionation. *Cell and Tissue Research* **1998,** *293*, 365 - 373.

29. Ehrlich, H.; Ilan, M.; Maldonado, M.; Muricy, G.; Bavestrello, G.; Kljajic, Z.; Carballo, J.; Schiaparelli, S.; Ereskovsky, A.; Schupp, P., Three-dimensional chitin-based scaffolds from Verongida sponges (Demospongiae: Porifera). Part I. Isolation and identification of chitin. *International Journal of Biological Macromolecules* **2010,** *47*, (2), 132-140.

30. Kosyakov, V. N.; Yakovlev, N. G.; Veleshko, I. E., Application of chitin-containing fiber material "Mycoton" for actinide absorption. *Journal of Nuclear Science and Technology* **2002,** *39*, 508-511.

31. LLorens, I.; Solari, P. L.; Sitaud, B.; Bes, R.; Cammelli, S.; Hermange, H.; Othmane, G.; Safi, S.; Moisy, P.; Wahu, S.; Bresson, C.; Schlegel, M. L.; Menut, D.; Bechade, J.-L.; Martin, P.; Hazemann, J.-L.; Proux, O.; Den Auwer, C., X-ray absorption spectroscopy investigations on radioactive matter using MARS beamline at SOLEIL synchrotron. *Radiochimica Acta* **2014**, *102*, 957-972.

32. Sitaud, B.; Solari, P. L.; Schlutig, S.; Llorens, I.; Hermange, H., Characterization of radioactive materials using the MARS beamline at the synchrotron SOLEIL. *Journal of Nuclear Materials* **2012,** *425*, (1–3), 238-243.

33. Ravel, B.; Newville, M., ATHENA, ARTEMIS, HEPHAESTUS: data analysis for X-ray absorption spectroscopy using IFEFFIT. *Journal of synchrotron radiation* **2005,** *12*, (4), 537-541.

34. Meihaus, K. R.; Minasian, S. G.; Lukens, W. W., Jr.; Kozimor, S. A.; Shuh, D. K.; Tyliszczak, T.; Long, J. R., Influence of pyrazolate vs N-heterocyclic carbene ligands on the slow magnetic relaxation of homoleptic trischelate lanthanide(III) and uranium(III) complexes. *J Am Chem Soc* **2014,** *136*, (16), 6056-68.

35. Löble, M. W.; Keith, J. M.; Altman, A. B.; Stieber, S. C.; Batista, E. R.; Boland, K. S.; Conradson, S. D.; Clark, D. L.; Lezama Pacheco, J.; Kozimor, S. A.; Martin, R. L.; Minasian, S. G.; Olson, A. C.; Scott, B. L.; Shuh, D. K.; Tyliszczak, T.; Wilkerson, M. P.; Zehnder, R. A., Covalency in Lanthanides. An X-ray Absorption Spectroscopy and Density Functional Theory Study of LnCl6(x-) (x = 3, 2). *J Am Chem Soc* **2015,** *137*, (7), 2506-23.

36. Hitchcock, A., aXis2000 is written in Interactive Data Language (IDL). *It is available free for noncommercial use from* http://unicorn. *mcmaster. ca/aXis2000. html* **2008**.